

Measuring Plasma Parameters With Thermal Noise Spectroscopy

Nicole Meyer-Vernet, Sang Hoang, Karine Issautier, Milan Maksimovic, Robert Manning,
and Michel Moncuquet

DESPA/CNRS ura 264, Observatoire de Paris, Meudon, France

Robert G. Stone

NASA/Goddard Space Flight Center, Greenbelt, Maryland

This paper describes the basic principles, the unique features and the limitations of thermal noise spectroscopy as a tool for *in situ* diagnostics in space plasmas. This technique is based on the analysis of the electrostatic field spectrum produced by the quasi-thermal fluctuations of the electrons and ions, which can be measured with a sensitive wave receiver at the terminals of an electric antenna. This method produces routine measurements of the bulk electron density and temperature, and is being extended to measure the ion bulk speed. It has the advantage of being in general relatively immune to spacecraft potential and photoelectron perturbations, since it senses a large plasma volume. We compare this method to other techniques, and give examples of applications in the solar wind as well as in cometary and in magnetized planetary environments.

1. INTRODUCTION

Since particles and electrostatic waves are so closely coupled in a plasma, particle properties can be determined by measuring waves. In a stable plasma, the particle thermal motions produce electrostatic fluctuations which are completely determined by the velocity distributions (and the static magnetic field) [Rostoker, 1961]. Hence, this quasi-thermal noise, which can be measured with a sensitive receiver at the terminals of an electric antenna, allows *in situ* plasma measurements.

Except near magnetized planets, the electron gyrofrequency f_g is much smaller than the plasma frequency f_p . Then, the electron thermal motions excite Langmuir waves, so that the quasi-equilibrium spectrum is

cut-off at f_p , with a peak just above it (see Figure 1). In addition, the electrons passing closer than a Debye length L_D to the antenna induce voltage pulses on it, producing a plateau in the wave spectrum below f_p and a decreasing level above f_p ; since L_D is mainly determined by the bulk (core) electrons, so are these parts of the spectrum. In contrast, since the Langmuir wave phase velocity $v_\phi \rightarrow \infty$ as $f \rightarrow f_p$, the fine shape of the f_p peak is determined by the high-velocity electrons.

Hence when $f_g \ll f_p$, measuring the thermal noise spectrum allows a precise determination of the electron density and bulk temperature (using respectively the cut-off at f_p and the spectrum level and shape around it), whereas the detailed shape of the peak itself reveals the suprathermal electrons (see [Meyer-Vernet and Perche, 1989] and references therein). This technique, first introduced in the solar wind [Meyer-Vernet, 1979; Couturier *et al.*, 1981; Kellogg, 1981], has been applied in a cometary tail [Meyer-Vernet *et al.*, 1986a, b], in the Earth's plasmasphere [Lund *et al.*, 1994], and in the interplanetary medium over a wide range of heliocen-

tric distances and latitudes [Hoang *et al.*, 1992, 1996; Maksimovic *et al.*, 1995; Issautier *et al.*, 1997].

In the environment of magnetized planets the effect of the ambient magnetic field is not negligible and the technique must be modified accordingly; this modification is outlined in Section 5.

2. BASICS

2.1. Theory

The voltage power spectrum of the plasma quasi-thermal noise at the terminals of an antenna in a plasma drifting with velocity \mathbf{V} is

$$V_{\omega}^2 = \frac{2}{(2\pi)^3} \int d^3k \left| \frac{\mathbf{k} \cdot \mathbf{J}}{k} \right|^2 E^2(\mathbf{k}, \omega - \mathbf{k} \cdot \mathbf{V}) \quad (1)$$

The first term in the integral involves the antenna response to electrostatic waves, which depends on the Fourier transform $\mathbf{J}(\mathbf{k})$ of the current distribution along the antenna. The second term is the autocorrelation function of the electrostatic field fluctuations in the antenna frame. At frequencies $f \gg f_g$, we have

$$E^2(\mathbf{k}, \omega) = 2\pi \frac{\sum_j q_j^2 \int d^3v f_j(\mathbf{v}) \delta(\omega - \mathbf{k} \cdot \mathbf{v})}{k^2 \epsilon_0^2 |\epsilon_L(\mathbf{k}, \omega)|^2} \quad (2)$$

$f_j(\mathbf{v})$ being the velocity distribution of the j^{th} species of charge q_j , and $\epsilon_L(\mathbf{k}, \omega)$ the plasma longitudinal dielectric function (see for example [Sitenko, 1967]).

For a wire dipole antenna made of two thin filaments each of length L along the x axis we have [Kuehl, 1966]

$$\mathbf{k} \cdot \mathbf{J} = 4 \frac{\sin^2(k_x L/2)}{k_x L} \quad (3)$$

This expression assumes that the current decreases linearly with distance along each antenna arm, or equivalently, that the measured voltage is the difference between the voltages averaged over each arm. This is expected to hold in general if the filament radius is much smaller than the electrostatic wave-lengths, and if $\omega L/c \ll 1$ [Schiff, 1971]. The signal at the ports of a receiver is $V_R^2 = V_{\omega}^2 \times |Z_R / (Z_R + Z_A)|^2$, where the receiver impedance Z_R is mainly due to the antenna base capacitance, and the antenna impedance Z_A is given by

$$Z_A(\omega) = \frac{i}{(2\pi)^3 \omega \epsilon_0} \int d^3k \left| \frac{\mathbf{k} \cdot \mathbf{J}}{k} \right|^2 \frac{1}{\epsilon_L(\mathbf{k}, \omega - \mathbf{k} \cdot \mathbf{V})} \quad (4)$$

2.2. Measuring the Electron Density and Bulk Temperature, and Estimating the Hot Component

Eq.(3) shows that a thin wire dipole antenna is mainly sensitive to wave vectors whose projection along its direction is of the order of π/L . This result has important consequences [Meyer-Vernet and Perche, 1989]. First, in order to be well adapted to observe Langmuir waves (which satisfy $k < 1/L_D$), the antenna length should exceed a few Debye lengths. Second, if $\pi V/L \ll \omega_p$ (where $V = |\mathbf{V}|$), the Doppler shift is negligible for waves observed near f_p (this statement is also true if V is much smaller than the particle thermal velocities); thus the ion contribution to Eq.(2) is negligible near f_p , since f_p is much larger than the ion characteristic frequencies.

This condition generally holds in the near-ecliptic low-speed interplanetary medium, in cometary environments, and in the outer plasmasphere. A diagnostic of electrons is then obtained from the noise measured around f_p by [Meyer-Vernet and Perche, 1989]:

- assuming a model of the velocity distribution,
- calculating the electron quasi-thermal spectrum from Eqs.(1) to (4),
- deducing the parameters of the model by fitting the result to the observations.

Figure 1 shows a typical example of such a fitting, obtained with the 2×35 -m wire dipole antenna of the URAP experiment [Stone *et al.*, 1992a] on Ulysses in the in-ecliptic solar wind. The electron distribution is described by a superposition of a cold (c) plus a hot (h) Maxwellian [Feldman *et al.*, 1975], and the fitting yields the electron total density n , cold temperature T_c , and the ratios n_h/n_c , T_h/T_c . The precision is much better for the total density (a few per cent) and core temperature (generally better than 15 %) than for the hot population because an accurate diagnostic of suprathermal particles would require measuring the spectral peak with a very good frequency resolution [Chateau and Meyer-Vernet, 1989, 1991].

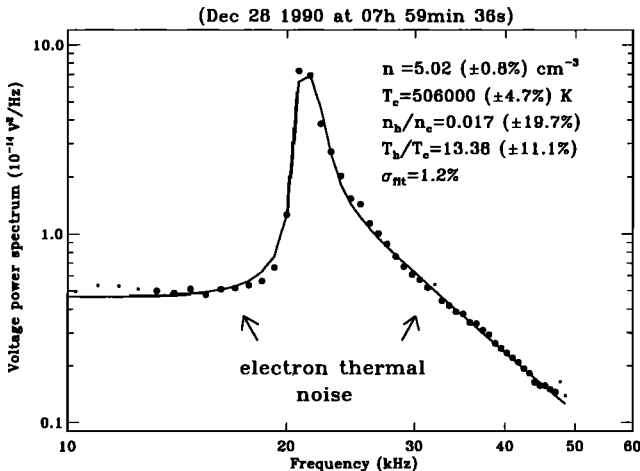


Figure 1. Example of voltage power spectrum measured by URAP on Ulysses in the solar wind (dots) and the deduced plasma parameters. The solid curve is the theoretical electron quasi-thermal noise, with the best-fit parameters indicated. (The statistical uncertainties are obtained from the fitting procedure.)

2.3. Measuring the Ion Bulk Speed

When the bulk speed is not negligible, as in the interplanetary medium when $\pi V/L \ll \omega_p$, the above method can be used to measure it. Since the proton and electron thermal velocities are respectively much smaller and much larger than V , the bulk velocity has no significant effect on the electron thermal noise, but the proton noise is strongly Doppler-shifted, so that it is no longer negligible, especially for $f < f_p$ [Meyer-Vernet *et al.*, 1986c]. In that case, the proton bulk speed can be deduced by fitting the theoretical electron-plus-proton noise to the observed spectrum [Issautier *et al.*, 1996].

This situation is illustrated in Figure 2 which is based on data obtained with the URAP wire dipole antenna on Ulysses. The fitting yields the proton bulk speed V (and temperature), in addition to the electron parameters n , T_c , n_h/n_c , T_h/T_c [Issautier *et al.*, 1996]. In the present preliminary state of the method, which is not yet fully optimized, the precision on V is generally 10-20%; (in addition, the precision on T_c is better than when the drift velocity is neglected). The method is not well suited to measure the proton temperature T_p since the spectrum is in general sensitive to T_p only at very low frequencies where the shot noise produced by particle impacts and photoemission on the antenna is large.

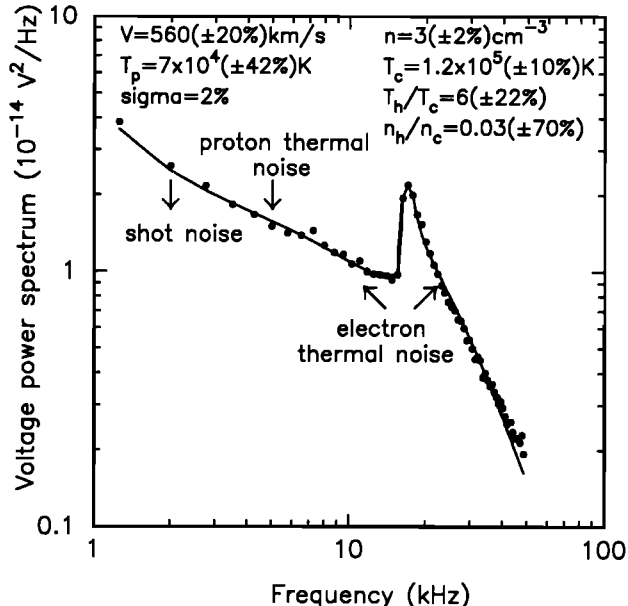


Figure 2. Example of voltage power spectrum measured by URAP on Ulysses in the solar wind when the Doppler-shifted proton contribution is important (dots) and the deduced plasma parameters. The solid curve is the theoretical electron-plus-proton quasi-thermal noise (plus the shot noise, which is only significant at the smallest frequencies). The best-fit parameters are shown.

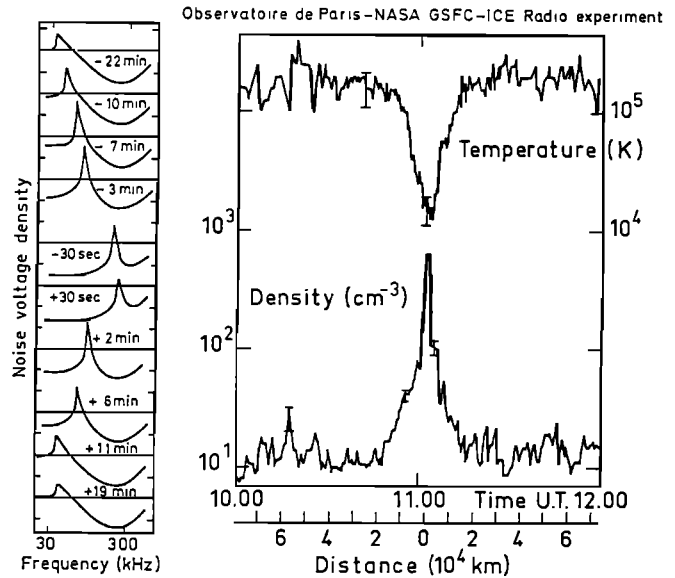


Figure 3. A series of thermal noise spectra recorded by the radio experiment aboard ICE during the crossing of the tail of comet Giacobini-Zinner, and the corresponding profiles of electron density and temperature as a function of the distance from the tail axis at 7800 km from the nucleus. (adapted from [Meyer-Vernet *et al.*, 1986a])

3. EXAMPLES OF APPLICATION

3.1. Cometary Electrons

This technique was first used on a large scale with the radio experiment on the spacecraft ISEE-3/ICE when it crossed the tail of comet Giacobini-Zinner (Figure 3). The experiment yielded the profiles of cometary electron density and temperature during the encounter. These results are unique because the ICE electrostatic electron analyzer could not detect adequately the cold cometary electrons in the plasma sheet ($n = 670 \text{ cm}^{-3}$, $T = 1.3 \times 10^4 \text{ K}$) as the effects of the spacecraft potential and photoelectrons could not be properly eliminated.

3.2. Solar Wind

Plate 1 shows an example of routine plasma measurement with the Ulysses URAP experiment. The upper panel is a radio spectrogram displayed as frequency versus time, i.e., the time evolution of spectra such as shown in Figure 2. The high level near 20 kHz corresponds to quasi-thermal Langmuir waves, close to f_p , which gives the plasma density. The bottom panel shows the density, core electron temperature and bulk speed deduced from the fittings. The structure shown corresponds to Ulysses crossing an interplanetary shock.

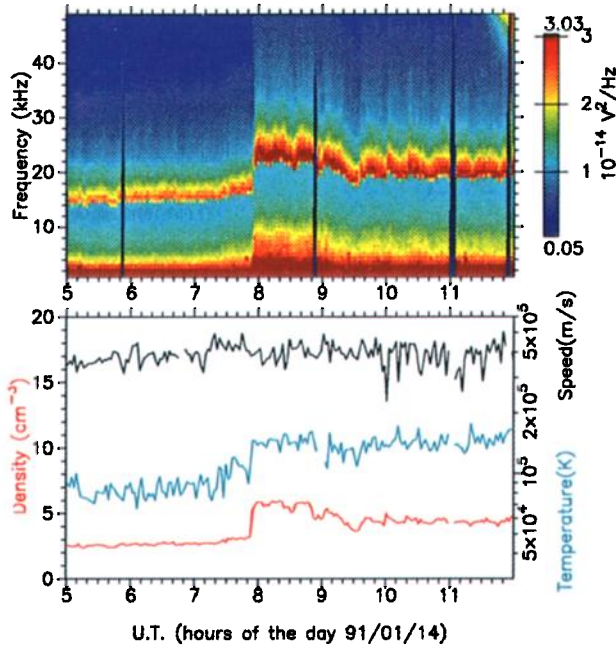


Plate 1. Example of routine plasma measurements obtained from quasi-thermal noise spectroscopy in the interplanetary medium. The upper panel is a radio spectrogram plotted as frequency versus time, with relative intensity indicated by the color bar chart on the right. The bottom panel shows the electron density, core temperature, and bulk speed deduced from the data.

4. WHY AND WHEN DOES IT WORK?

4.1. Comparison With Other Techniques

The presence of several instruments measuring electron parameters aboard Ulysses made possible an extensive comparison between them. The electron density was measured by:

- the SWOOPS electron analyzer [Bame et al., 1992],
- thermal noise spectroscopy with the URAP radio receiver [Stone et al., 1992a],
- the URAP relaxation sounder [Stone et al., 1992a].

Maksimovic et al. [1995] compared 12,000 nearly simultaneous measurements (acquired within 1 minute of separation) from SWOOPS and from the thermal noise at several heliocentric distances in the ecliptic; the SWOOPS densities were on average 19% smaller than the thermal noise ones. A comparison was then made with improved SWOOPS results obtained with a vectorial correction of spacecraft charging effects [Scime et al., 1994]; these densities are closer to the thermal noise ones, i.e., only 13% smaller (Figure 4(a)). In contrast, the density measurements from the sounder and from the thermal noise differ by only $(6 \pm 3)\%$ (Figure 4(b)).

These results suggest that, although the vectorial correction of spacecraft charging effects improves the results of the Ulysses electron analyzer, it still underes-

timates the density by about 10%. The core electron temperature aboard Ulysses was measured by both the electron analyzer and thermal noise spectroscopy. The results are within 17% of each other (Figure 4(c)).

4.2. Advantages, Drawbacks, and Design

The above Sections illustrated the main advantages of thermal noise spectroscopy:

- the large volume sensed: since the Langmuir wavelength satisfies $\lambda_L > 2\pi L_D$, the antenna is equivalent to a sensor of surface $S > 2\pi L_D \times L$, making the method in general relatively immune to spacecraft potential and photoelectron perturbations,
- the simplicity of density measurements (in general one has just to locate a frequency on a spectrogram, and this works even in presence of strong radioemissions since electromagnetic waves do not propagate below f_p), and their independence of gain calibration.

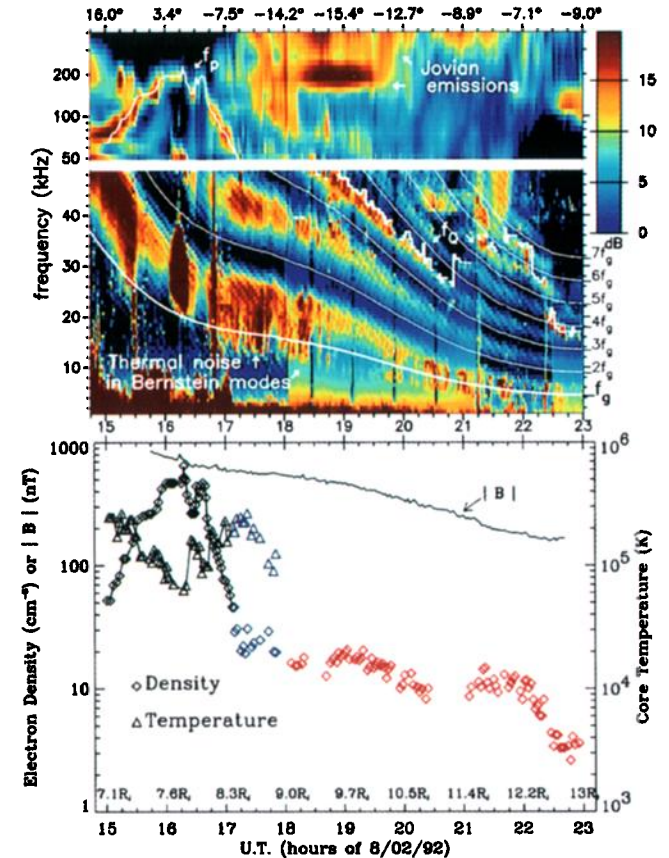


Plate 2. Upper panel: Radio spectrogram measured by URAP on Ulysses in the Io plasma torus and beyond. Lower panel: Corresponding electron density, bulk temperature, and magnetic field $|B|$, deduced from quasi-thermal noise analysis, as a function of time, Jovicentric distance (bottom scale), and magnetic latitude (top scale of upper panel). The color symbols refer to different measurement methods.

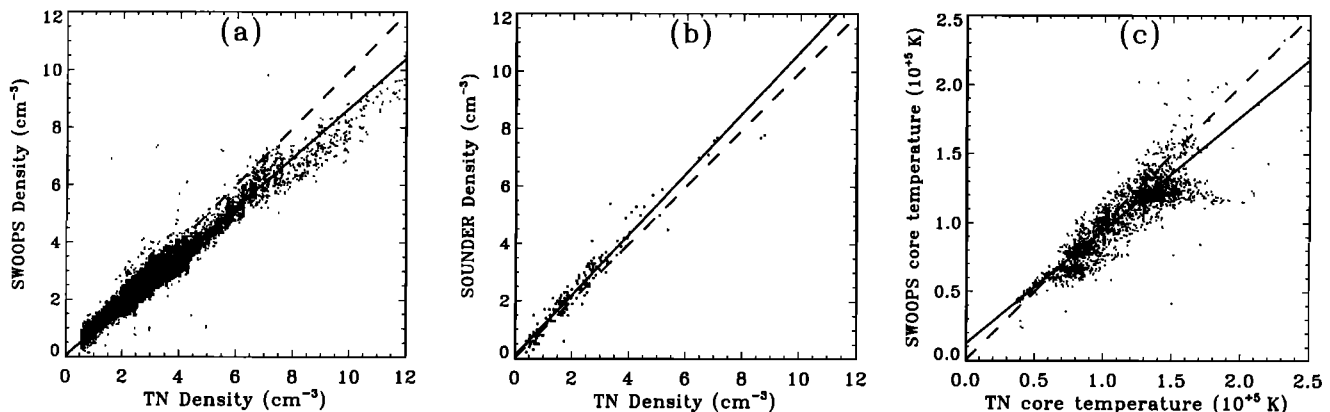


Figure 4. Scatter plot of electron density measurements from the thermal noise (TN) and (a) the electrostatic analyzer SWOOPS on Ulysses or (b) the URAP sounder. In each case, the continuous line corresponds to the line that minimizes the perpendicular dispersion from it and a dotted line of slope 1 is superimposed. (c) Scatter plot of electron temperature measurements from the thermal noise and the electrostatic analyzer, with the same kind of associated lines. (adapted from [Maksimovic *et al.*, 1995]).

In contrast, as already noted, the method is not well-adapted to measure suprathermal particles. In addition, as most wave measurements of bulk plasma parameters, it is perturbed by strong plasma instabilities.

For the method to work, the following conditions have to be met:

- the antenna length must exceed a few L_D in order to detect adequately the Langmuir wave cut-off and peak,
- the antenna must be sufficiently thin in order (i) to minimize the shot noise and (ii) have a radius smaller than L_D (for the simple theory used to hold),
- a good frequency resolution is necessary to resolve the peak,
- a sensitive and well-calibrated receiver is required in order to measure the temperature accurately; this condition is not necessary to obtain the density, which can be measured even with receivers of moderate sensitivity (see [Gurnett *et al.*, 1979; Lund *et al.*, 1994]).

5. MAGNETIZED PLASMA

When the electron gyrofrequency f_g is not negligible compared to f_p , the wave spectrum around f_p is modified by the electron gyration in the magnetic field. In that case, the electron thermal motion excites Bernstein waves, and the observed quasi-thermal noise shows weak bands with well-defined minima at gyroharmonics below the upper-hybrid band [Meyer-Vernet *et al.*, 1993], peaks at the upper-hybrid f_{UH} and f_Q frequencies [Christiansen *et al.*, 1978], and drops in the frequency bands where no Bernstein waves propagate [Moncuquet *et al.*, 1997].

The minima at gyroharmonics allow a simple measurement of the modulus of the magnetic field. Plate 2 shows an application on Ulysses in the Io plasma torus; this determination agrees with the magnetometer results

within a few percent [Meyer-Vernet *et al.*, 1993]. In addition, the quasi-thermal noise levels at maxima yield an estimate of the hot electron temperature [Sentman, 1982].

The f_{UH} and f_Q peaks can yield the total electron density [see for example Birmingham *et al.*, 1981; Hoang *et al.*, 1993] (black diamonds in Plate 2). The density can also be deduced from the signal disappearances in the Bernstein wave forbidden bands [Moncuquet *et al.*, 1997] (red symbols); on Ulysses these results were in agreement with the few measurements given by the relaxation sounder [Stone *et al.*, 1992b]. Note however that the accuracy of all these density measurements may be limited by the possibility of confusion between different resonance frequencies, especially in the non-equilibrium case.

The bulk temperature can be obtained either (i) from the thermal noise level at the minima, or (ii) by measuring the Bernstein wave-length (black triangles in Plate 2) [Meyer-Vernet *et al.*, 1993; Moncuquet *et al.*, 1995]. Method (ii) requires a spinning spacecraft; it is based on the fact that the angular pattern of the antenna is a sensitive function of kL when $kL \geq 1$ (see Eq.(3) and [Meyer-Vernet, 1994]), so that measuring the thermal noise spin modulation yields k . This technique requires a wire dipole antenna longer than the electron gyroradius r_g , since Bernstein waves have $k \sim 1/r_g$. In addition to the bulk electron temperature, this can also yield an estimate of the density (blue symbols in Plate 2).

6. CONCLUSION AND PERSPECTIVES

Thermal noise spectroscopy is complementary to electrostatic analyzers to measure accurately the density and the bulk electron temperature when spacecraft pho-

toelectron and charging effects cannot be properly eliminated. This method requires a sensitive receiver and a wire dipole antenna; it is routinely used on Ulysses and has been implemented on Wind; it will also be used on Cassini, and is proposed on several future missions.

REFERENCES

- Bame, S. J. *et al.*, The Ulysses solar wind plasma experiment, *Astron. Astrophys. Suppl. Ser.*, *92*, 237-265, 1992.
- Birmingham, T. J., J. K. Alexander, M. D. Desch, R. F. Hubbard, and B. M. Pedersen, Observations of electron gyroharmonic waves and the structure of Io torus, *J. Geophys. Res.*, *86*, 8497-8507, 1981.
- Chateau, Y. F, and N. Meyer-Vernet, Electrostatic noise in Non-Maxwellian plasmas: "Flat-Top" distribution function, *J. Geophys. Res.*, *94*, 15,407-15,414, 1989.
- Chateau, Y. F, and N. Meyer-Vernet, Electrostatic noise in Non-Maxwellian plasmas: Generic properties and Kappa distributions, *J. Geophys. Res.*, *96*, 5825, 1991.
- Christiansen, P. J. *et al.*, Geos-I observations of electrostatic waves, and their relationship with plasma parameters, *Space Sci. Rev.*, *22*, 383-400, 1978.
- Couturier, P., S. Hoang, N. Meyer-Vernet, and J.-L. Steinberg, Quasi-thermal noise in a stable plasma at rest, *J. Geophys. Res.*, *86*, 11,127-11,138, 1981.
- Feldman, W. C., J. R. Asbridge, S. J. Bame, M. D. Montgomery, and S. P. Gary, Solar wind electrons, *J. Geophys. Res.*, *80*, 4181-4196, 1975.
- Gurnett, D. A., R. R. Anderson, F. L. Scarf, R. W. Fredericks, and E. J. Smith, Initial results from the ISEE-1 and -2 plasma wave investigation, *Space Sci. Rev.*, *23*, 103-122, 1979.
- Hoang, S. *et al.*, Solar wind thermal electrons in the ecliptic plane between 1 and 4 AU: preliminary results from the Ulysses radio receiver, *Geophys. Res. Lett.*, *19*, 1295-1298, 1992.
- Hoang, S., N. Meyer-Vernet, M. Moncuquet, A. Lecacheux, and B. M. Pedersen, Electron density and temperature in the Io plasma torus from Ulysses thermal noise measurements, *Planet. Space Sci.*, *41*, 1011-1020, 1993.
- Hoang, S., N. Meyer-Vernet, K. Issautier, M. Maksimovic, M. Moncuquet, Latitude dependence of solar wind plasma thermal noise: Ulysses radio observations, *Astron. Astrophys.*, *316*, 430-434, 1996.
- Issautier, K., N. Meyer-Vernet, M. Moncuquet, and S. Hoang, A novel method to measure the solar wind speed, *Geophys. Res. Lett.*, *23*, 1649-1652, 1996.
- Issautier, K., N. Meyer-Vernet, M. Moncuquet, and S. Hoang, Pole to pole solar wind density from Ulysses radio measurements, *Solar Phys.*, in press, 1997.
- Kellogg, P., Calculation and observation of thermal electrostatic noise in solar wind plasma, *Plasma Phys.*, *23*, 735-751, 1981.
- Kuehl, H. H., Resistance of a short antenna in a warm plasma, *Radio Sci.*, *1*, 971-976, 1966.
- Lund, E. J., J. Labelle, and R. A. Treumann, On quasi-thermal fluctuations near the plasma frequency in the outer plasmasphere: a case study, *J. Geophys. Res.*, *99*, 23,651-23,660, 1994.
- Maksimovic, M. *et al.*, The solar wind electron parameters from quasi-thermal noise spectroscopy, and comparison with other measurements on Ulysses, *J. Geophys. Res.*, *100*, 19,881-19,891, 1995.
- Meyer-Vernet, N., On natural noises detected by antennas in plasmas, *J. Geophys. Res.*, *84*, 5373-5377, 1979.
- Meyer-Vernet, N., On the thermal noise "temperature" in an anisotropic plasma, *Geophys. Res. Lett.*, *21*, 397, 1994.
- Meyer-Vernet, N. *et al.*, Plasma diagnosis from quasi-thermal noise and limits on dust flux or mass in comet Giacobini-Zinner, *Science*, *232*, 370-374, 1986a.
- Meyer-Vernet, N., P. Couturier, S. Hoang, C. Perche, J.L. Steinberg, Physical parameters for hot and cold electron populations in comet Giacobini-Zinner, *Geophys. Res. Lett.*, *13*, 279-282, 1986b.
- Meyer-Vernet, N., P. Couturier, S. Hoang, J.L. Steinberg, and R. D. Zwickl, Ion thermal noise in the solar wind: interpretation of the "excess" electric noise on ISEE 3, *J. Geophys. Res.*, *91*, 3294-3298, 1986c.
- Meyer-Vernet, N., and C. Perche, Tool kit for antennae and thermal noise near the plasma frequency, *J. Geophys. Res.*, *94*, 2405-2415, 1989.
- Meyer-Vernet, N., S. Hoang, and M. Moncuquet, Bernstein waves in the Io plasma torus: a novel kind of electron temperature sensor, *J. Geophys. Res.*, *98*, 21,163-21,176, 1993.
- Moncuquet, M., N. Meyer-Vernet, and S. Hoang, Dispersion of electrostatic waves in the Io plasma torus and derived electron temperature, *J. Geophys. Res.*, *100*, 21,697-21,708, 1995.
- Moncuquet, M. N. Meyer-Vernet, S. Hoang, R. J. Forsyth, and P. Canu, Detection of Bernstein wave forbidden bands: a new way to measure the electron density, *J. Geophys. Res.*, *102*, 2373-2379, 1997.
- Rostoker, N., Fluctuations of a plasma, *Nucl. Fusion*, *1*, 101-120, 1961.
- Schiff, M. L., Current distribution on a grid type dipole antenna immersed in a warm isotropic plasma, *Radio Sci.*, *6*, 665-671, 1971.
- Scime, E. E., J. L. Phillips, and S. J. Bame, Effects of spacecraft potential on three-dimensional electron measurements in the solar wind, *J. Geophys. Res.*, *99*, 14,769-14,776, 1994.
- Sentman, D. D., Thermal fluctuations and the diffuse electrostatic emissions, *J. Geophys. Res.*, *87*, 1455, 1982.
- Sitenko, A. G., *Electromagnetic Fluctuations in Plasma*, Academic, San Diego, Calif., 1967.
- Stone, R. G. *et al.*, The Unified Radio and Plasma Wave Investigation, *Astron. Astrophys. Suppl. Ser.*, *92*, 291-316, 1992a.
- Stone, R. G. *et al.*, Ulysses radio and plasma wave observations in the Jupiter environment, *Science*, *257*, 1524-1531, 1992b.

S. Hoang, K. Issautier, M. Maksimovic, R. Manning, N. Meyer-Vernet, M. Moncuquet, DESPA, Observatoire de Paris, 92195 Meudon Cedex, France. e-mail: meyer@obsppm.fr

R. G. Stone, NASA/GSFC, Greenbelt, MD 20771, USA.